American Journal of Climate Change, 2025, 14(3), 605-625
https://www.scirp.org/journal/ajcc
ISSN Online: 2167-9509
ISSN Print: 2167-9495

# Evaluating Structure-from-Motion Photogrammetry for Dendrometric Measurements of Trees in Agro-Sylvopastoral Landscapes

**Moussa Diédhiou[1], Omar Sarr[1], Abdoul Aziz Diouf[2], Tamsir Mbaye[3], Ousmane Ndiaye[4], Sékouna Diatta[1], Daouda Ngom[1]**

[1]Department of Plant Biology, Faculty of Science and Technology, University Cheikh Anta Diop, Dakar, Senegal
[2]Centre de Suivi Ecologique (CSE), Dakar, Senegal
[3]National Center for Forestry Research (CNRF), Senegalese Agricultural Research Institute (ISRA), Dakar, Senegal
[4]Zootechnical Research Center, Senegalese Agricultural Research Institute (ISRA), Dakar, Senegal
Email: moussaddh732@gmail.com

**How to cite this paper:** Diédhiou, M., Sarr, O., Diouf, A. A., Mbaye, T., Ndiaye, O., Diatta, S., & Ngom, D. (2025). Evaluating Structure-from-Motion Photogrammetry for Dendrometric Measurements of Trees in Agro-Sylvopastoral Landscapes. *American Journal of Climate Change, 14,* 605-625.
https://doi.org/10.4236/ajcc.2025.143029

**Received:** May 20, 2025
**Accepted:** August 9, 2025
**Published:** August 12, 2025



## Abstract

Recent applications of Structure-from-Motion (SfM) photogrammetry in forestry have highlighted its robustness in tree mensuration. This study proposes an optimized image acquisition protocol for generating high-quality 3D point clouds of individual trees of *Faidherbia albida* (Delile) A.Chev and *Acacia tortilis* haynes ssp. raddiana (Savi) Brenan with varying sizes and forms in a Sahelian agrosilvopastoral system in Senegal. A measurement protocol adapted for estimating key dendrometric parameters was established, including tree height, crown diameter, and diameter at breast height (DBH, 1.30 m). A Mavic Pro drone and a TG-5 ground camera were used to photograph 20 individuals of each species. Acquired georeferenced images were processed using Metashape 1.5.1 trial version to produce dense 3D point clouds. Depending on tree isolation and height, models were reconstructed either from drone images alone or from a combination of aerial and ground images. The dendrometric parameters were estimated with high precision. DBH was measured with an nRMSE of 6% and Bias values of −1.3 and −0.04 for *F. albida* and *A. tortilis*, respectively. Total tree height was estimated with nRMSEs of 9% and 12%, and Bias values of −0.04 and 0.41. Crown diameter showed nRMSEs of 9% and 0.10%, with Bias values of 0.57 and 0.85, respectively. This study demonstrated the effectiveness of combining drone and ground-based pictures for accurate 3D reconstruction and measurement of dendrometric parameters on individual trees in Sahelian landscapes. The proposed protocol will be useful for assessing carbon sequestration and for developing climate change mitigation strategies

in Sahelian ecosystems.

## Keywords

SfM, Trees, Agrosilvopastoral, DBH, Height, Crown, Sahel

## 1. Introduction

The effects of climate change remain a major concern for Africa, particularly for the Sahelian region of West Africa, which is severely affected by drought (GIS-Climat, 2012). Since the late 1970s, temperatures have risen by 0.2˚C to 0.8˚C per decade across the Sahelo-Saharan, Sahelian, and Sudanian zones (CILSS, 2010; GIEC, 2007). This temperature increase has led to considerable variability in rainfall at both seasonal and decadal scales (Heinrigs, 2010; Morel, 1998; Nicholson, 2005; Sircoulon, 1976), disrupting production systems and threatening the livelihoods of agropastoral communities, who are highly vulnerable to climatic hazards (CILSS, 2010; Nouaceur et al., 2013). Moreover, ecosystems in the region are experiencing increasing degradation due to the combined effects of natural and human factors, including monoculture, bushfires, and overgrazing (Dugué et al., 2012; Guisse et al., 2013; Ozer et al., 2010).

Like other Sahelian countries, Senegal is undergoing profound ecological changes, characterized by decreasing water resources and more frequent droughts (MEDD, 2016). These changes have negative impacts on agriculture and are contributing to the depletion of forage resources. According to the Ministry of Environment and Sustainable Development (MEDD, 2016), 70% of pastoral households may abandon their activity by 2030 due to the increasing severity of droughts. In response, several adaptation strategies have been implemented to strengthen the resilience of local populations. These include the Plan Sénégal Émergent (PSE), early warning systems (SAP), and the Tessékéré International Human-Environment Observatory (OHMi). These initiatives promote the adoption of sustainable agricultural systems based on selected plant species, such as *Faidherbia albida* (Del.) Chev. agroforestry parks (MEDD, 2016), forage potential assessments in pastoral areas (Diouf et al., 2014), and the valorization of drought-resistant species such as Faidherbia albida and *Acacia tortilis* haynes ssp. raddiana (Savi) Brenan, particularly in northern Ferlo and the Senegalese groundnut basin (Diouf et al., 2014; Guisse et al., 2013).

These species play a central role in Senegalese agroecosystems: they provide fodder for livestock, enhance soil fertility and microclimate conditions (Dendoncker & Vincke, 2015; Diedhiou et al., 2014; Kuyah et al., 2016; Miller et al., 2017; Reed et al., 2017; Sinare & Gordon, 2015), and offer significant carbon sequestration potential (Adamou et al., 2020; Alexandre et al., 2020; Jaiswal et al., 2014; Laminou Manzo et al., 2015). Given the numerous ecological and socio-economic benefits of these woody species, optimizing their sustainable management is essential.

Such optimization is particularly relevant for implementing effective carbon sequestration strategies. In this context, the availability of accurate data, including tree volume, is a key requirement. These data are critical for developing reliable tools to estimate woody volumes and biomass, while ensuring the preservation and sustainability of forest stands.

Traditionally, data are collected manually in the field with a labor-intensive process that is often prone to measurement errors. Precision forestry, enabled by recent advances in remote sensing (RGB photogrammetry and LiDAR), now offers a scalable alternative (Lisein et al., 2014). Structure from Motion (SfM) photogrammetry converts a series of 2D images into detailed 3D models (Astrup et al., 2014; Gatziolis et al., 2015; Tinkham & Swayze, 2021; Zhou & Zhang, 2020). This cost-effective method can be implemented using drones, cameras, or even smartphones [29, 33]. In the Sahel, this technique has already been used to characterize tree height and crown structure in the Ferlo region (Bossoukpe et al., 2021; Talla, 2021) and to assess the influence of *Faidherbia albida* on crop performance in agroforestry systems (Roupsard et al., 2020). However, current protocols do not capture the trunk or allow for the direct estimation of woody volume.

To address this gap, our study proposes an improved image acquisition and analysis protocol using SfM photogrammetry tailored to the 3D reconstruction of both the trunk and crown of Sahelian trees. The method combines aerial drone imagery with ground-based photography, using a circular capture pattern around each sampled tree. This integrated approach aims to enable the low-cost estimation of aboveground biomass in a more complete and accurate manner.

## 2. Materials and Methods

### 2.1. Study Sites

The study was conducted at two sites located in contrasting ecosystems: the agricultural peanut basin of Niakhar in the Fatick region and the Sahelian sylvopastoral zone of Dahra in the Louga region (**Figure 1**).

**Niakhar/Sob Agroforestry Park:** This site is located in the central-western region of Senegal (Fatick region), within an agro-silvo-pastoral system dominated by bush fields and family-run farms (Niakhar: −16.452864, 14.495134 UTM 28N). The soils are Arenosols, according to the FAO classification, with a sandy loam or coarser texture and less than 20% clay content (Delon et al., 2022). Between 1981 and 2021, the average annual rainfall was 589 mm (range: 279.5 - 965 mm), and the average air temperature was 27.5˚C (range: 26.3˚C - 28.4˚C). The measured average tree density is 6.8 individuals per hectare, with a marked dominance of *Faidherbia albida*, reaching an average height of 13.3 m.

**Dahra Sylvopastoral Zone (CRZ Dahra):** The second site is located in the northwestern region of Senegal (Louga region), within a Sahelian pastoral zone (CRZ: −15.39608, 15.37701 UTM 28N). The climate is Sahelian, with a short rainy season from July to September, sometimes extending into October. Between 1981 and 2021, the annual rainfall was 431 mm (range: 163.0 - 938 mm), and the average

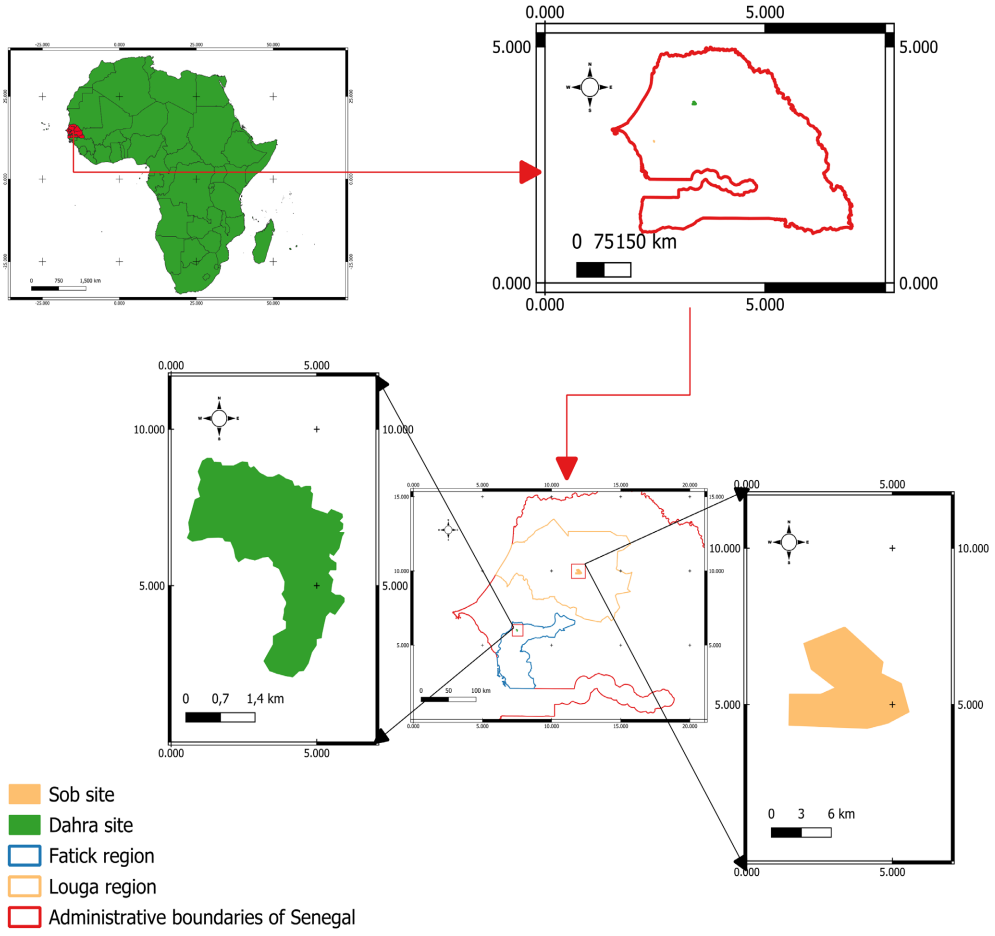


**Figure 1.** Geolocation map of the Niakhar (Fatick) and Dahra (Louga) study sites.

annual temperature was 27.85˚C (range: 26.98˚C - 28.75˚C). The soils are very sandy (89% sand, 6.3% clay), with a pH ranging from 6.2 to 7.4 in the upper horizon (Delon et al., 2022). The woody vegetation consists of native tree species such as *Balanites aegyptiaca*, *Acacia senegal*, *Boscia senegalensis*, *Acacia tortilis* subsp. *raddiana*, and *Acacia seyal* var. seyal. The measured average tree height is 4.4 m, with a total basal area of 2.1 $m^2 \cdot ha^{-1}$ and an average tree density of 13.9 $trees \cdot ha^{-1}$.

## 2.2. Drone Image Acquisition

In this study, Aerial images were acquired using a DJI Mavic Pro drone. This ultra-compact multi-rotor drone (83 × 83 × 198 $mm^3$, <800 g) is equipped with a 3-axis stabilized camera capable of recording 4K UHD video at up to 30 frames per second and Full HD 1080p at up to 96 fps. It also captures 12-megapixel still images in JPEG or DNG RAW format. The gimbal can tilt up to 90˚, allowing flexible capture angles adapted to various topographic and structural contexts (Studiosport, 2022).

Additionally, ground-based photos were taken using an Olympus TG-5 digital camera. This compact device (113 × 66 × 31.9 $mm^3$, 250 g) is equipped with a 12-

megapixel 1/2.33" CMOS sensor. It features a 3-inch LCD screen with a resolution of 460,000 pixels and an ISO range of 100 to 12,800 (LDLC, 2022). The TG-5 also includes multiple embedded sensors (GPS, compass, barometer, thermometer, and level indicator), which enhance its capacity to gather contextual environmental data for analysis.

### 2.3. Drone Flight Plan

For each individual tree, approximately 400 images were captured. Prior to each flight, local conditions were systematically checked, particularly wind speed, lighting, and ambient temperature, as these factors can significantly influence image quality. A circular flight path was then executed around each tree at a constant speed of 0.9 m/s.

Additionally, a three-dimensional scale reference composed of three 1-meter rods (X, Y, Z) was placed near each tree, but outside the canopy area.

The image acquisition protocol consisted of nadir photographs captured from above the canopy, complemented by several circular image sequences taken around individual trees at a 45˚ oblique angle, in order to better capture the tree structure from multiple perspectives:

- Altitude 30 m, circular path with a 15 m radius;
- Altitude 20 m, circular path with a 15 m radius;
- Altitude 10 m, circular path with a 15 m radius;
- Altitude 5 m, circular path with a 15 m radius.

**During the capture phase, the gimbal was tilted at 45˚, and image overlap was maintained between 70% and 80%.**

### 2.4. Ground-Based Photographs

Ground photography is particularly important in the case of non-isolated trees, where surrounding obstacles hinder full capture by drone (Miller et al., 2015). To address this limitation, complementary ground photography was systematically carried out.

After drone flights, approximately 200 ground-based images were captured for each sampled tree using the Olympus TG-5 camera, set to auto mode for ISO and exposure adjustment, which is essential under highly variable Sahelian lighting conditions. The ground capture protocol was organized around two concentric circles around each tree:

**Circle 1** (maximum distance Dmax allowing the entire tree to fit in the frame):

- Photos were taken every 20˚ (about two steps) around the tree.

**Circle 2** (Dmax/2, i.e., halfway between the tree and Circle 1):

- Photos were taken every 10˚ (about one step) around the tree.

At each position, three vertically overlapping shots were captured (70% - 80% overlap):

- Angle 1: reference + ground + trunk.
- Angle 2: trunk + base of the crown.

- Angle 3: upper crown.

This acquisition scheme ensures complete coverage of the trunk and canopy, thereby optimizing the quality of the resulting 3D models.

## 2.5. Plant Material

The study focused on *Faidherbia albida*, for the agroforestry parks of Niakhar, and on *Acacia tortilis*, for the sylvopastoral zone. These two species represent a diversity of structures and architectures, as well as variations in size and morphology; we selected individuals belonging to different circumference classes. A total of 20 trees were photographed for each species. The breast height circumference classes and the number of samples are presented in Table 1.

**Table 1.** Sampling of *Faidherbia albida* and *Acacia tortilis* individuals according to circumference classes.

| *Faidherbia albida* | | *Acacia tortilis* | |
|---|---|---|---|
| Circumference | Number of samples | Circumference | Number of samples |
| [93.98 - 130.83) | 2 | [9.82 - 38.5) | 7 |
| (130.83 - 167.46) | 5 | (38.5 - 67.0) | 6 |
| (167.46 - 204.1) | 6 | (67.0 - 95.5) | 3 |
| (204.1 - 240.73) | 4 | (95.5 - 124.0) | 2 |
| (240.73 - 277.36) | 2 | (124.0 - 152.5) | 1 |
| (277.36 - 314.0] | 1 | (152.5 - 181.0] | 1 |

## 2.6. Processing of Aerial and Ground Images

### 2.6.1. Selection of Images

This analysis aims to produce a clean and accurate model for the measurement of dendrometric parameters. This approach allows for the reconstruction of camera positions from overlapping images, followed by the generation of a sparse point cloud, and then a dense point cloud (Akpo et al., 2020). Image processing was carried out considering two scenarios:

**Isolated tree**

For trees with few or no nearby obstacles, the 3D reconstruction was performed exclusively using drone-captured images. In this case, the viewing angles provided by the various altitudes and inclinations were sufficient to fully reconstruct both the trunk and the crown.

**Non-isolated tree**

When obstacles such as neighboring trees or branches limit aerial perspectives, 3D reconstruction required a combination of drone images with ground-based pictures. The analysis involved importing all drone and ground images into two separate folders before processing them. The resulting 3D models were subsequently merged using a few reference points (markers) to create a final model that better represents the tree. For some individuals, however, the ground-based im-

ages alone were sufficient to reconstruct a detailed 3D model, especially when aerial visibility was minimal or obstructed.

Ultimately, this approach allowed a complete and accurate reconstruction of the lower part of trees, which is often poorly captured by drone images alone. The distribution of images per individual is highlighted in **Table A1** in the appendix.

### 2.6.2. Images Processing

The image analysis was performed using Agisoft Metashape Professional (trial version v1.5.1). This software employs the Structure from Motion (SfM) method to simultaneously estimate camera parameters and orientations for each overlapping image pair, generating a sparse point cloud representing matching features within the photographic dataset. Subsequently, multi-view stereo algorithms are applied to the sparse point cloud to produce a dense point cloud, which can be converted into a textured three-dimensional model (Akpo et al., 2020).

Initially, images are grouped and sorted to remove duplicates and blurred images. The image quality within a chunk is assessed based on sharpness, exposure, focus, resolution, and depth of field. Images with a quality index less than or equal to 0.5 are discarded to facilitate alignment.

The 3D space scaling process involves selecting approximately ten images where the scale reference is clearly visible. On each of these images, pairs of markers are manually added to represent each axis (X, Y, and Z) of the reference, specifying their dimension (1 m). Since the drone images are georeferenced, Metashape automatically positions the corresponding markers on the remaining images, which are then reviewed and adjusted as necessary.

Following this, the image alignment phase was conducted considering four parameters:

- Accuracy;
- Generic preselection;
- Point limit;
- Tie point limit.

In this study, alignment was performed at a high accuracy level, whereas point densification was carried out at medium accuracy. Due to computational constraints, medium accuracy was chosen for camera positioning. As the camera operated in automatic mode during image acquisition, the "Generic" pair preselection mode was used to match common features across image pairs. Default parameters were applied for the number of key points and tie points, set at 150,000 and 10,000, respectively.

### 2.6.3. Scaling of 3D Models and Dendrometric Parameters Measurement

To enable accurate measurements on the 3D models, the 3D space was scaled. A set of about ten images where the three-dimensional scale reference (X, Y, Z) was clearly visible was selected. A pair of markers was manually added to each image to represent the axes and their dimensions (1 meter per axis). Leveraging the

georeferencing system, Metashape automatically propagates these markers across the entire image set. However, a manual verification is subsequently carried out to correct any potential discrepancies.

### 2.6.4. Photographs and Field Measurements

The photographic capture and field measurement campaigns were conducted in two distinct periods, specifically in December 2021 for *Faidherbia albida* and in February 2022 for *Acacia tortilis*. These periods were selected because they coincide with the leafing phase of each species, a favorable condition for optimal capture of the canopy.

The dendrometric parameters measured on-site include the diameter at 1.30 m from the ground (DBH), measured using a tape measure; the total tree height, determined using a Blume-Leiss instrument; and the canopy cross diameters measured with a tape measure. These measurements allow for the validation of the estimates derived from the 3D models (Figure 2).

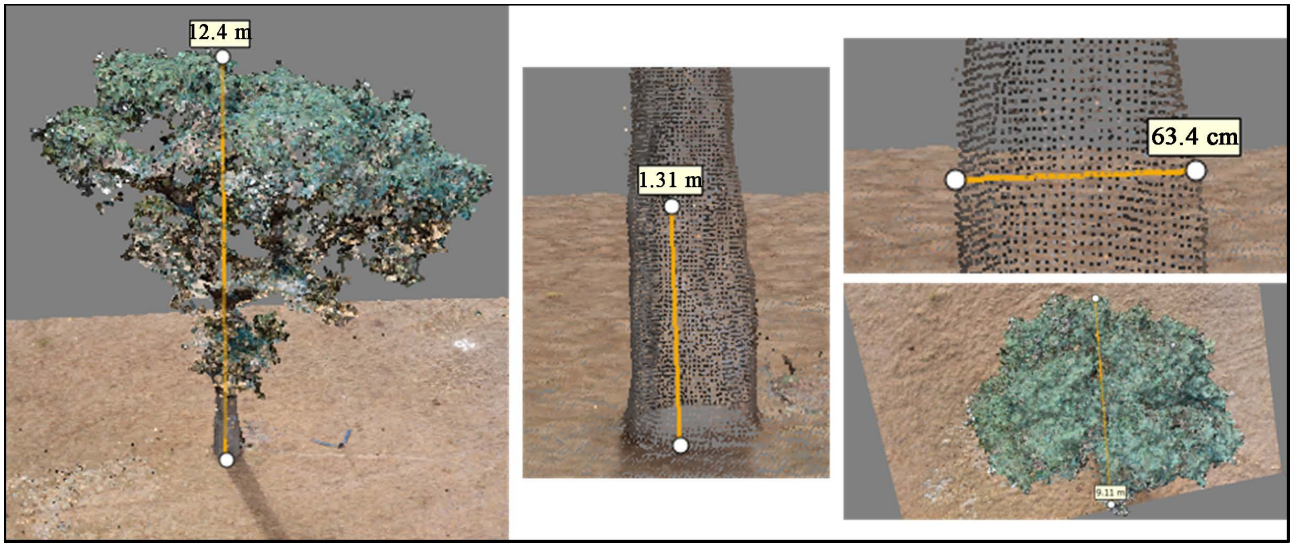


**Figure 2.** Measurement of tree dendrometric parameters using Metashape.

### 2.6.5. Validation of Estimated Dendrometric Parameters

The agreement between field measurements and estimates derived from 3D models was assessed by fitting a 1:1 relationship, supported by statistical indicators including root mean squared error (RMSE), normalized RMSE (nRMSE), Bias, and Efficiency Factor (EF). Rather than relying on internal photogrammetric metrics (e.g., reprojection errors), the evaluation focused on the accuracy of dendrometric parameters extracted from the models, which served as indirect indicators of reconstruction quality.

$$\mathrm{RMSE} = \sqrt{\frac{1}{n}\sum_{i=1}^{n}\left(y_i - \hat{y}_i\right)^2} \quad (1)$$

$$\mathrm{nRMSE} = \frac{\mathrm{RMSE}}{\hat{y}} \times 100 \quad (2)$$

$$\text{Bias} = \frac{1}{n}\sum_{i=1}^{n}\left(y_i - \hat{y}_i\right) \quad (3)$$

$$\text{EF} = \frac{\sum_{i=1}^{n}\left(y_i - \hat{y}_i\right)^2}{\sum_{i=1}^{n}\left(y_i - \bar{y}\right)^2} \quad (4)$$

## 3. Results and Discussion

### 3.1. 3D Reconstruction of Trees

Figure A1 and Figure A2 (see Appendix) present the results of the tree reconstruction. A point cloud was successfully generated for all individuals of Faidherbia albida and *Acacia tortilis*, respectively. Upon closer inspection of the tree components in the generated models, it was observed that, for the trunk, 90% of the 3D models were correctly reconstructed with a complete 3D model, characterized by a homogeneous distribution of points along the X, Y, and Z axes, accurately capturing the shape of the trunk. In contrast, 10% of the models were flattened, displaying a heterogeneous distribution of points concentrated only along the x and y axes.

The canopy reconstructions yielded similar patterns. For Faidherbia albida, 18 models (90%) exhibited complete point clouds, representing both the trunk and the crown with consistent spatial coverage, while 2 models (10%) were sparse, with a heterogeneous distribution of points across all three axes and numerous gaps, resulting in a discontinuous representation of the crown. For Acacia tortilis, 16 models (80%) were complete, and 4 models (20%) were flattened, with limited vertical structure in the point cloud.

### 3.2. Evaluation of Dendrometric Parameters

Table 2 below highlights the statistical validation variables between field and estimated dendrométric parameters using SfM 3D models. Analysis of this table shows that the trunk diameter at 1.30 m above ground, total height, and canopy diameter of individuals from both species were estimated with nRMSE ranging between 6% and 12%. Specifically, the trunk diameter was estimated with nRMSE of 6% for *Faidherbia albida* and *Acacia tortilis*. The total height was estimated with nRMSE of 9% and 12% while the canopy diameter was estimated with nRMSE of 8% and 10% respectively. Moreover, Figure 3 shows the validation line

Table 2. Statistical validation parameters between field measurements and SfM-derived estimates. TD (cm): Trunk diameter, TH (m): Tree height and CD (m): crown diameter.

| | *Faidherbia albida* | | | | | *Acacia tortilis* | | | | |
|---|---|---|---|---|---|---|---|---|---|---|
| | RMSE | nRMSE | nBias | Bias | EF | EMSE | nRMSE | nBias | Bias | EF |
| **TD** | 4.05 | 0.006 | −0.02 | −1.3 | 0.93 | 3.1 | 0.06 | −0.04 | −1.83 | 0.95 |
| **TH** | 0.63 | 0.09 | −0.01 | −0.04 | 0.91 | 0.85 | 0.12 | 0.06 | 0.41 | 0.81 |
| **CD** | 0.86 | 0.08 | 0.05 | 0.57 | 0.88 | 1.2 | 0.1 | 0.07 | 0.85 | 0.89 |

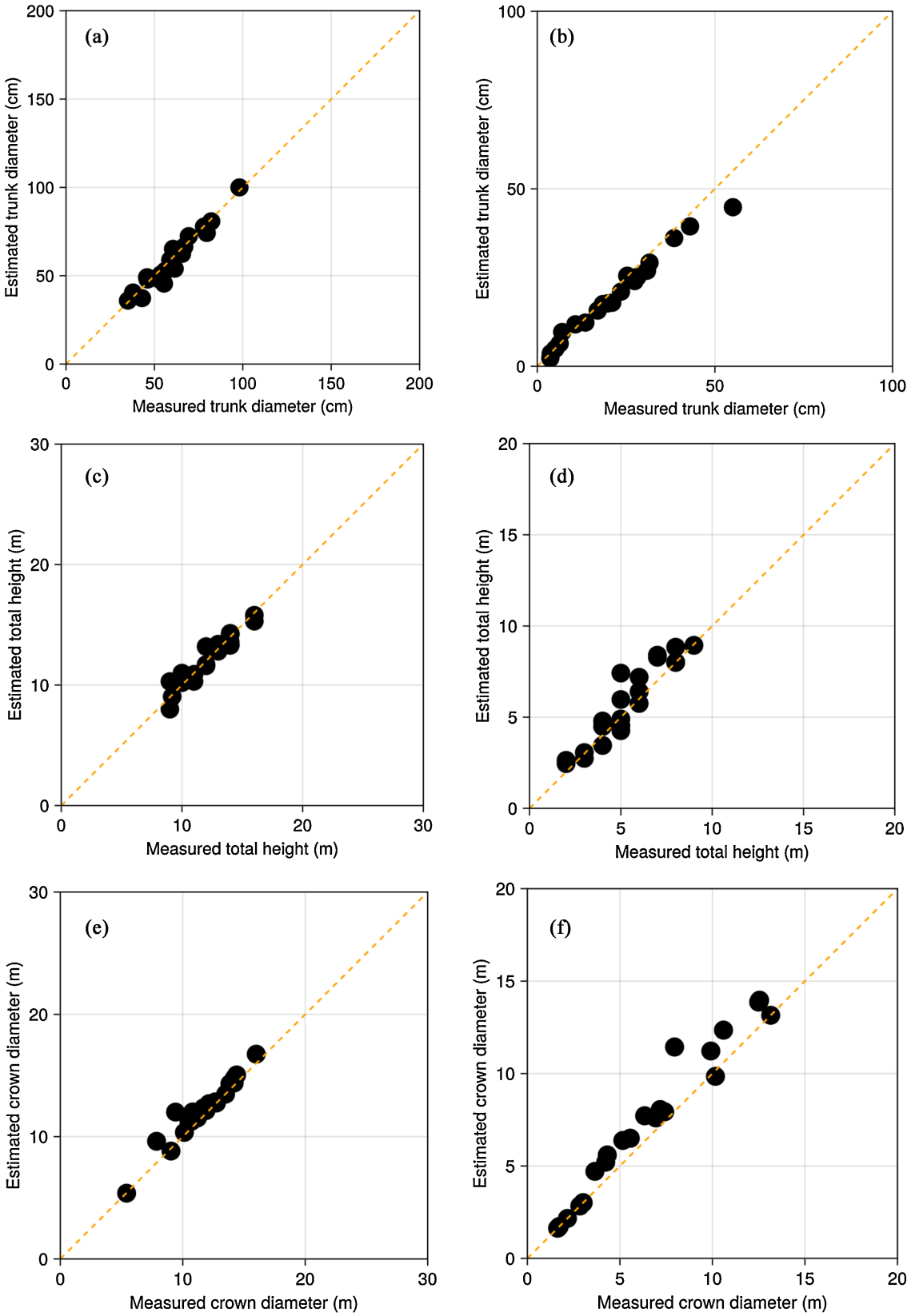


**Figure 3.** 1:1 line fitting between observed and estimated dendrometric parameters. DBH (a), (b), total height (c), (d) and crown diameter (e), (f). (a), (c) and (e) are *Faidherbia albida*; (b), (d) and (f) are *Acacia tortilis*.

between the different field measurements and those derived from the SfM models. A fairly homogeneous distribution was observed around the 1:1 line.

### 3.3. Image Optimization

The optimization was conducted on three complete 3D models (EC12, EC13 and EC16), derived from drone images, where trees were not subject to occlusion issues. **Figure A3** and **Figure A4** (see Appendix) show the position of raw and the optimized images used for the reconstruction of identical point clouds of an individual tree. **Figure A5** (see Appendix) presents the residual errors of the tie points between initial and optimized models. Approximately 300 to 400 images were initially used to reconstruct a tree, and the optimization was carried out as follows:

- Retain three (3) photo circles and the nadir photos of the canopy from above.
- Remove every other image in each circle, while ensuring that the remaining images retain a sufficient overlap of 70% - 80% to maintain alignment and reconstruction quality.

Then, a high-resolution 3D model, identical to the one initially produced with raw images, was reconstructed using around 120 photos. Specifically, starting from the bottom to the top, the first and second circles consisted of 30 photos each, while the third circle, centered on the canopy, included 43. The total average alignment error (projection of tie points on X, Y, and Z) for EC12, EC13 and EC16 is slightly lower for the optimized model (92.34 cm) compared to the initial model (95.99 cm) (**Table 3**).

**Table 3.** Average camera location error. X: Longitude, Y: Latitude, Z: Altitude for EC12, EC13 and EC16 models.

| Models | Average X (cm) | Average Y (cm) | Average Z (cm) | Average error XY (cm) | Average total error (cm) |
|---|---|---|---|---|---|
| Initial | 18.35 | 27.51 | 90.11 | 33.08 | 95.99 |
| Optimized | 32.98 | 26.8 | 81.98 | 42.49 | 92.34 |

### 3.4. Discussion

The application of Structure-from-Motion (SfM) techniques in forestry has opened new possibilities for the detailed characterization of stands and individual trees (Akpo et al., 2020; Gatziolis et al., 2015; Iglhaut et al., 2019). With the advancements in multi-view photogrammetry (MVS), it is now possible to reconstruct 3D models of trees with acceptable precision in measuring biophysical parameters (Dong et al., 2020; Guerra-Hernández et al., 2017; Gülci, 2019). In this study, we implemented a combined methodology using drone and ground-based photography, adapted to the agro-sylvopastoral ecosystems of Senegal. The results show that the quality of 3D reconstruction strongly depends on whether the trees are isolated or not. We worked on individuals belonging to different circumference classes in automatic exposure mode to minimize lighting bias.

At the end of the reconstruction phase, 90% of isolated trees produced complete

3D models, while 10% of non-isolated trees produced partial models affected by occlusion. These results corroborate the observations of (Miller et al., 2015) and (Sakai et al., 2021), who showed that isolated trees enable high-resolution 3D modeling, unlike trees in dense stands, where occlusion limits model quality.

The validation of parameters (diameter at 1.30 m, total height, canopy diameter) showed low error rates:

- For Faidherbia albida: nRMSE of 6% (diameter), 9% (height), 8% (canopy).
- For *Acacia tortilis*, nRMSE of 6%, 12%, and 10% respectively.

These performances align with those obtained by (Miller et al., 2015) (error of 3.74% on height, 9.6% on diameter at 1.3 m, and 11.93% on canopy) and also match the results of (Bossoukpe et al., 2021) and (Talla et al., 2020) for tree height estimation in the Senegalese Ferlo region (RMSE error of 0.97 m and 0.44 m, respectively).

The creation of accurate and complete 3D point cloud models of individual trees provides a strong basis for the indirect estimation of woody biomass. By integrating these models into Quantitative Structure Models (QSMs) (Dong et al., 2021), it becomes possible to fit cylinders along all structural components of the tree trunks, branches, and forks, thereby enabling detailed volume and biomass assessments. Compared to LiDAR-based approaches, which remain costly and less accessible in many regions, this low-cost photogrammetric solution offers a promising alternative for large-scale biomass estimation. Importantly, it reduces the need for destructive sampling of trees traditionally used to develop allometric equations.

In the context of climate change, such advances in 3D modeling are particularly crucial for Sahelian ecosystems, where rising temperatures, changing rainfall patterns, and increasing land degradation threaten the stability of agro-sylvopastoral landscapes. Accurate assessment of woody biomass and carbon stocks at the individual tree and stand level supports better monitoring of carbon dynamics and ecosystem health under climate-driven stress. These methods thus provide essential tools to inform sustainable forest management and carbon sequestration strategies that aim to mitigate climate impacts in vulnerable dryland regions.

However, a larger error was observed in the estimation of trunk diameter, especially for non-isolated trees. This error appears to be linked to scaling uncertainties during the merging of drone and ground models, a phenomenon also highlighted by Tinkham & Swayze (2021). These authors showed that the quality of the point cloud is influenced by the Metashape processing pipeline, notably the chosen resolution and the type of filtering applied (aggressive vs. minimal filtering). They also demonstrated that larger trees (>7 m) are reconstructed with high quality, while understory trees present more errors.

Nonetheless, our results on trunk diameter are comparable to recent work by Bayati et al. (2021) and Kim et al. (2019), who found estimation errors of 2.17 cm and 1.99 cm, respectively, for trunk diameter.

Furthermore, our optimization of the number of images showed that a robust 3D model could be obtained with only 120 drone images for an isolated tree, with

a reduction in alignment error (92.34 cm compared to 95.99 cm for the full model). This confirms the observations of Miller et al. (2015), who stated that a single sensor is sufficient to model an isolated tree. However, for non-isolated trees, ground-based photogrammetry remains essential to fill in the gaps caused by occlusion.

This issue is at the heart of recent work on continuous ground-based photogrammetry, aimed at extending 3D modeling to the scale of entire plots despite structural obstacles. Liu et al. (2018), for example, managed to achieve mean squared errors of 3.07% to 4.51% on trunk diameter in complex forest environments.

Meanwhile, Gao & Kan (2022) developed an automated pipeline (Auto-DBH) for quickly estimating trunk diameter (DBH) on three forest plots, with very low errors (1.41 cm, 1.118 cm, and 3.16 cm according to the plots). These recent works show that it is now possible to design semi-automated acquisition and processing pipelines for detailed large-scale modeling, including in Sahelian contexts.

## 4. Conclusion

The creation of a realistic 3D point cloud is highly dependent on the morphology of tree crowns, their size, and the density of the surrounding stand. These factors not only influence the selection of sensors and the number of images to capture, but also affect the complexity and reliability of the photogrammetric processing workflow. In agroforestry parklands and sylvopastoral landscapes of Senegal, where stand density remains relatively moderate, the photogrammetric reconstruction of individual trees benefits from favorable conditions for application.

However, field sampling sometimes revealed challenging cases, such as contiguous trees or individuals with atypical architectures. In these situations, a combined approach using both drone and ground-based imagery proved necessary to achieve an acceptable 3D reconstruction, especially when aiming to visualize occluded parts like trunks or lower crowns. Isolated and tall trees were generally easier to reconstruct from UAV images alone, whereas non-isolated individuals required systematic integration of terrestrial images to better capture their lower structures.

Some limitations were encountered, particularly with several trees (e.g., Faidherbia albida and Acacia tortilis), where reconstruction was affected by occlusion, low image overlap, or model deformation. The variability in point cloud quality and the residual alignment errors observed highlight the importance of acquisition geometry and camera calibration.

Despite these constraints, Structure-from-Motion (SfM) photogrammetry enabled the extraction of dendrometric parameters such as total tree height, crown diameter, and trunk diameter with a level of precision that is acceptable for silvicultural applications in this context. Our objective was not to reach geodetic-level accuracy but to evaluate whether this approach could deliver usable structural information for ecological and forestry monitoring.

All trees were analyzed using a standardized processing workflow, with me-

dium-quality settings and aggressive depth filtering parameters that directly affected both processing time and model density. The resulting 3D models offer promising opportunities for:

- Silvicultural planning and resource management.
- Estimating stem taper coefficients.
- Approximating total tree volume.
- And, potentially, modeling aboveground biomass at multiple spatial scales.

In addition to these direct applications, the use of SfM photogrammetry for generating high-resolution 3D models of trees is highly relevant in the context of climate change. In Sahelian ecosystems where rising temperatures, erratic rainfall, and land degradation are intensifying, an accurate monitoring of woody biomass and vegetation structure is crucial to assess the resilience and carbon sequestration potential of agro-sylvopastoral systems. SfM photogrammetry provides a non-destructive, scalable, and repeatable method for evaluating climate-related impacts on tree architecture, thereby supporting adaptation strategies and sustainable land management in vulnerable dryland regions.

## Acknowledgements

This work was supported by projects: 1) EU-funded DeSIRA CaSSECS (FOOD/2019/410-169) and 2) EU-funded Horizon 2020 SustainSAHEL project (Grant No. 861974). We would like to thank the PPZS "*Pôle Pastoralisme et Zones Sèches*" for their support during the fieldwork, in particular to Paulo Salgado, Mariama Diop and Mamadou Gassama.

## Conflicts of Interest

The authors declare no conflicts of interest regarding the publication of this paper.

## References

Adamou, S., Amani, A., Mahamadou, H. M., & Drame Yaye, A. (2020). Modèle allométrique d'estimation du carbone aérien séquestré par *Balanites aegyptiaca* (L.) Del dans la partie Sud-Ouest du Niger. *Afrique Science, 16,* 188-203. http://www.afriquescience.net

Akpo, H. A., Atindogbé, G., Obiakara, M. C., Adjinanoukon, A. B., Gbedolo, M., Lejeune, P. et al. (2020). Image Data Acquisition for Estimating Individual Trees Metrics: Closer Is Better. *Forests, 11,* Article No. 121. https://doi.org/10.3390/f11010121

Alexandre, T., Tchobsala, Amadou, M. L. M., Ahmadou, H., & Adamou, I. (2020). Species-Specific Allometric Equations for Predicting Biomass of *Faidherbia albida* (del.) A. Chev. in the Sudano-Sahelian Savannahs of Far-North, Cameroon. *Journal of Agriculture and Ecology Research International, 21,* 33-44. https://doi.org/10.9734/jaeri/2020/v21i630151

Astrup, R., Ducey, M. J., Granhus, A., Ritter, T., & von Lüpke, N. (2014). Approaches for Estimating Stand-Level Volume Using Terrestrial Laser Scanning in a Single-Scan Mode. *Canadian Journal of Forest Research, 44,* 666-676. https://doi.org/10.1139/cjfr-2013-0535

Bayati, H., Najafi, A., Vahidi, J., & Gholamali Jalali, S. (2021). 3D Reconstruction of Une-

ven-Aged Forest in Single Tree Scale Using Digital Camera and SfM-MVS Technique. *Scandinavian Journal of Forest Research, 36,* 210-220. https://doi.org/10.1080/02827581.2021.1903074

Bossoukpe, M., Faye, E., Ndiaye, O., Diatta, S., Diatta, O., Diouf, A. A. et al. (2021). Low-Cost Drones Help Measure Tree Characteristics in the Sahelian Savanna. *Journal of Arid Environments, 187,* Article ID: 104449. https://doi.org/10.1016/j.jaridenv.2021.104449

CILSS (2010). *Vulnérabilité, impacts et stratégies d'adaptation des populations locales à la variabilité et aux changements climatiques Comite permanent interetats de lutte contre la secheresse dans le sahel permanent inter-state committee for drought control in the sa*. 28.

Delon, C., Galy-Lacaux, C., Barret, B., Ndiaye, O., Serça, D., Guérin, F. et al. (2022). Nitrogen Budget and Critical Load Determination at a Sahelian Grazed Grassland Site. *Nutrient Cycling in Agroecosystems, 124,* 17-34. https://doi.org/10.1007/s10705-022-10220-6

Dendoncker, M., & Vincke, C. (2015). *Woody Resources Temporal Dynamics (1955-2015) and Radial Growth in the Ferlo (Senegal) as a Mean to Assess Ecosystem Stability*.

Diedhiou, M. A., Faye, E., Ngom, D., & Toure, M. A. (2014). Identification et caractérisation floristiques des parcs agroforestiers du terroir insulaire de Mar Fafaco (Fatick, Sénégal). *Journal of Applied Biosciences, 79,* 6855-6866. https://doi.org/10.4314/jab.v79i1.11

Diouf, A. A., Djaby, B., Diop, M. B., Wele, A., Ndione, J. A., & Tychon, B. (2014). *Fonctions d'ajustement pour l'estimation de la production fourragère herbacée des parcours naturels du Sénégal à partir du NDVI s10 de SPOT-Vegetation*.

Dong, X., Zhang, Z., Yu, R., Tian, Q., & Zhu, X. (2020). Extraction of Information about Individual Trees from High-Spatial-Resolution UAV-Acquired Images of an Orchard. *Remote Sensing, 12,* Article No. 133. https://doi.org/10.3390/rs12010133

Dong, Y., Fan, G., Zhou, Z., Liu, J., Wang, Y., & Chen, F. (2021). Low-Cost Automatic Reconstruction of Tree Structure by AdQSM with Terrestrial Close-Range Photogrammetry. *Forests, 12,* Article No. 1020. https://doi.org/10.3390/f12081020

Dugué, M., Delille, H., & de Capitalisation, S. M.-E. (2012). *Caractérisation des stratégies d'adaptation au changement climatique en agriculture paysanne*. Rop-pa-afrique.org.

Gao, Q., & Kan, J. (2022). Automatic Forest DBH Measurement Based on Structure from Motion Photogrammetry. *Remote Sensing, 14,* Article No. 2064. https://doi.org/10.3390/rs14092064

Gatziolis, D., Lienard, J. F., Vogs, A., & Strigul, N. S. (2015). 3D Tree Dimensionality Assessment Using Photogrammetry and Small Unmanned Aerial Vehicles. *PLOS ONE, 10,* e0137765. https://doi.org/10.1371/journal.pone.0137765

GIEC (2007). *Bilan 2007 des changements climatiques: Rapport de synthèse* (p. 114).

GIS-Climat (2012). *Regards croisés sur les enjeux du changement climatique en Afrique de l'Ouest climat environnement société* (p. 17).

Guerra-Hernández, J., González-Ferreiro, E., Monleón, V., Faias, S., Tomé, M., & Díaz-Varela, R. (2017). Use of Multi-Temporal UAV-Derived Imagery for Estimating Individual Tree Growth in Pinus Pinea Stands. *Forests, 8,* Article No. 300. https://doi.org/10.3390/f8080300

Guissé, A., Boëtsch, G., Ducourneau, A., Goffner, D., & Gueye, L. (2013). L'observatoire hommes-milieux international Tessékéré (OHMi): Un outil de recherche pour étudier la complexité des écosystèmes arides du Sahel. *Comptes Rendus. Biologies, 336,* 273-277. https://doi.org/10.1016/j.crvi.2013.04.007

Gülci, S. (2019). The Determination of Some Stand Parameters Using SfM-Based Spatial

3D Point Cloud in Forestry Studies: An Analysis of Data Production in Pure Coniferous Young Forest Stands. *Environmental Monitoring and Assessment, 191,* Article No. 495. https://doi.org/10.1007/s10661-019-7628-4

Heinrigs, P. (2010). *Incidences sécuritaires du changement climatique au Sahel: Perspectives Politiques*.

Iglhaut, J., Cabo, C., Puliti, S., Piermattei, L., O'Connor, J., & Rosette, J. (2019). Structure from Motion Photogrammetry in Forestry: A Review. *Current Forestry Reports, 5,* 155-168. https://doi.org/10.1007/s40725-019-00094-3

Jaiswal, D. G., Patel, N. C., Patel, B. Y., Mankad, U. A., & Pandya, A. H. (2014). Regression Correlation Analysis between GBH and Carbon Stock of Major Tree Species in Dharoi Range, Gandhinagar Forest Division, India. *International Journal of Innovative Research in Science, Engineering and Technology, 3,* 17146-17149. https://doi.org/10.15680/ijirset.2014.0311007

Kim, D.-S., Lee, D.-K., & Heo, H.-K. (2019). Estimation Carbon Storage of Urban Street Trees Using UAV Imagery and SfM Technique. *Journal of the Korean Society of Environmental Restoration Technology, 22,* 1-14. https://doi.org/10.13087/KOSERT.2019.22.6.1

Kuyah, S., Öborn, I., Jonsson, M., Dahlin, A. S., Barrios, E., Muthuri, C. et al. (2016). Trees in Agricultural Landscapes Enhance Provision of Ecosystem Services in Sub-Saharan Africa. *International Journal of Biodiversity Science, Ecosystem Services & Management, 12,* 1-19. https://doi.org/10.1080/21513732.2016.1214178

Laminou Manzo, O., Moussa, M., Issoufou, H. B., Abdoulaye, D., Morou, B., Youssifi, S. et al. (2015). Equations allométriques pour l'estimation de la biomasse aérienne de *Faidherbia albida* (Del.) Achev dans les agrosystèmes d'Aguié, Niger. *International Journal of Biological and Chemical Sciences, 9,* 1863-1874. https://doi.org/10.4314/ijbcs.v9i4.12

LDLC (2022). *LDLC—Olympus TG-5*. https://www.ldlc.com/fiche/PB00575063.html

Lisein, J., Bonnet, S., Lejeune, P., & Pierrot-Deseilligny, M. (2014). Modélisation de la canopée forestière par photogrammétrie depuis des images acquises par drone. *Revue Française de Photogrammétrie et de Télédétection, No. 206,* 45-54. https://doi.org/10.52638/rfpt.2014.7

Liu, J., Feng, Z., Yang, L., Mannan, A., Khan, T. U., Zhao, Z. et al. (2018). Extraction of Sample Plot Parameters from 3D Point Cloud Reconstruction Based on Combined RTK and CCD Continuous Photography. *Remote Sensing, 10,* Article No. 1299. https://doi.org/10.3390/rs10081299

MEDD (2016). *Echanges avec les Ministères sectoriels sur la CPDN/CDN* (p. 34).

Miller, D. C., Muñoz-Mora, J. C., & Christiaensen, L. (2017). Prevalence, Economic Contribution, and Determinants of Trees on Farms across Sub-Saharan Africa. *Forest Policy and Economics, 84,* 47-61. https://doi.org/10.1016/j.forpol.2016.12.005

Miller, J., Morgenroth, J., & Gomez, C. (2015). 3D Modelling of Individual Trees Using a Handheld Camera: Accuracy of Height, Diameter and Volume Estimates. *Urban Forestry & Urban Greening, 14,* 932-940. https://doi.org/10.1016/j.ufug.2015.09.001

Morel, R. (1998). Début de la sécheresse en Afrique de l'Ouest. In G. Demarée, J. Alexandre, & M. De Dapper (Eds.), *Tropical Climatology, Meteorology and Hydrology* (pp. 200-211). Royal Meteorological. Institute of Belgium/Royal Academy of Overseas Sciences.

Nicholson, S. (2005). On the Question of the "Recovery" of the Rains in the West African Sahel. *Journal of Arid Environments, 63,* 615-641. https://doi.org/10.1016/j.jaridenv.2005.03.004

Nouaceur, Z., Imen, T., & Benoıt, L. (2013). Changements climatiques au Sahel: Des conditions plus humides et plus chaudes en Mauritanie? *Sécheresse, 24,* 85-95.

Ozer, P., Hountondji, Y. C., Niang, A., Salifou, K., Manzo, O., & Salmon, M. (2010). Désertification au Sahel: Historique et perspectives. *Bulletin de la Société Géographique de Liège, 54,* 69-84.

Reed, J., van Vianen, J., Foli, S., Clendenning, J., Yang, K., MacDonald, M. et al. (2017). Trees for Life: The Ecosystem Service Contribution of Trees to Food Production and Livelihoods in the Tropics. *Forest Policy and Economics, 84,* 62-71. https://doi.org/10.1016/j.forpol.2017.01.012

Roupsard, O., Audebert, A., Ndour, A. P., Clermont-Dauphin, C., Agbohessou, Y., Sanou, J. et al. (2020). How Far Does the Tree Affect the Crop in Agroforestry? New Spatial Analysis Methods in a Faidherbia Parkland. *Agriculture, Ecosystems & Environment, 296,* Article ID: 106928. https://doi.org/10.1016/j.agee.2020.106928

Sakai, T., Birhane, E., Abebe, B., & Gebremeskel, D. (2021). Applicability of Structure-from-Motion Photogrammetry on Forest Measurement in the Northern Ethiopian Highlands. *Sustainability, 13,* Article No. 5282. https://doi.org/10.3390/su13095282

Sinare, H., & Gordon, L. J. (2015). Ecosystem Services from Woody Vegetation on Agricultural Lands in Sudano-Sahelian West Africa. *Agriculture, Ecosystems & Environment, 200,* 186-199. https://doi.org/10.1016/j.agee.2014.11.009

Sircoulon, J. (1976). *Les données hydropluviométriques de la sécheresse récente en Afrique intertropicale: Comparaison avec les sécheresses "1913" et "1940"-Fdi:14933-Horizon.*

Studiosport (2022). *Description Drone Mavic Pro.* https://www.studiosport.fr

Talla, R. (2021). *Etude de la végétation ligneuse au Ferlo (Sénégal) par une approche photogrammétrique, dendrométrie, dendrochronologie et évaluation de la séquestration du carbone chez Boscia senegalensis (Pers.) Lam. Ex Poir et Sclerocarya birrea. (A. Rich) Hoscht.* Université Cheikh ANTA DIOP.

Talla, R., Sagna, M. B., Diallo, M. D., Diallo, A., Ndiaye, D., Sarr, O. et al. (2020). Development of Allometric Models for Estimating the Biomass of *Sclerocarya birrea* (A. Rich) Hoscht and *Boscia senegalensis* (pers.) Lam. Ex Poir. *Open Journal of Ecology, 10,* 571-584. https://doi.org/10.4236/oje.2020.108035

Tinkham, W. T., & Swayze, N. C. (2021). Influence of Agisoft Metashape Parameters on UAS Structure from Motion Individual Tree Detection from Canopy Height Models. *Forests, 12,* Article No. 250. https://doi.org/10.3390/f12020250

Zhou, X., & Zhang, X. (2020). Individual Tree Parameters Estimation for Plantation Forests Based on UAV Oblique Photography. *IEEE Access, 8,* 96184-96198. https://doi.org/10.1109/access.2020.2994911

## Appendix

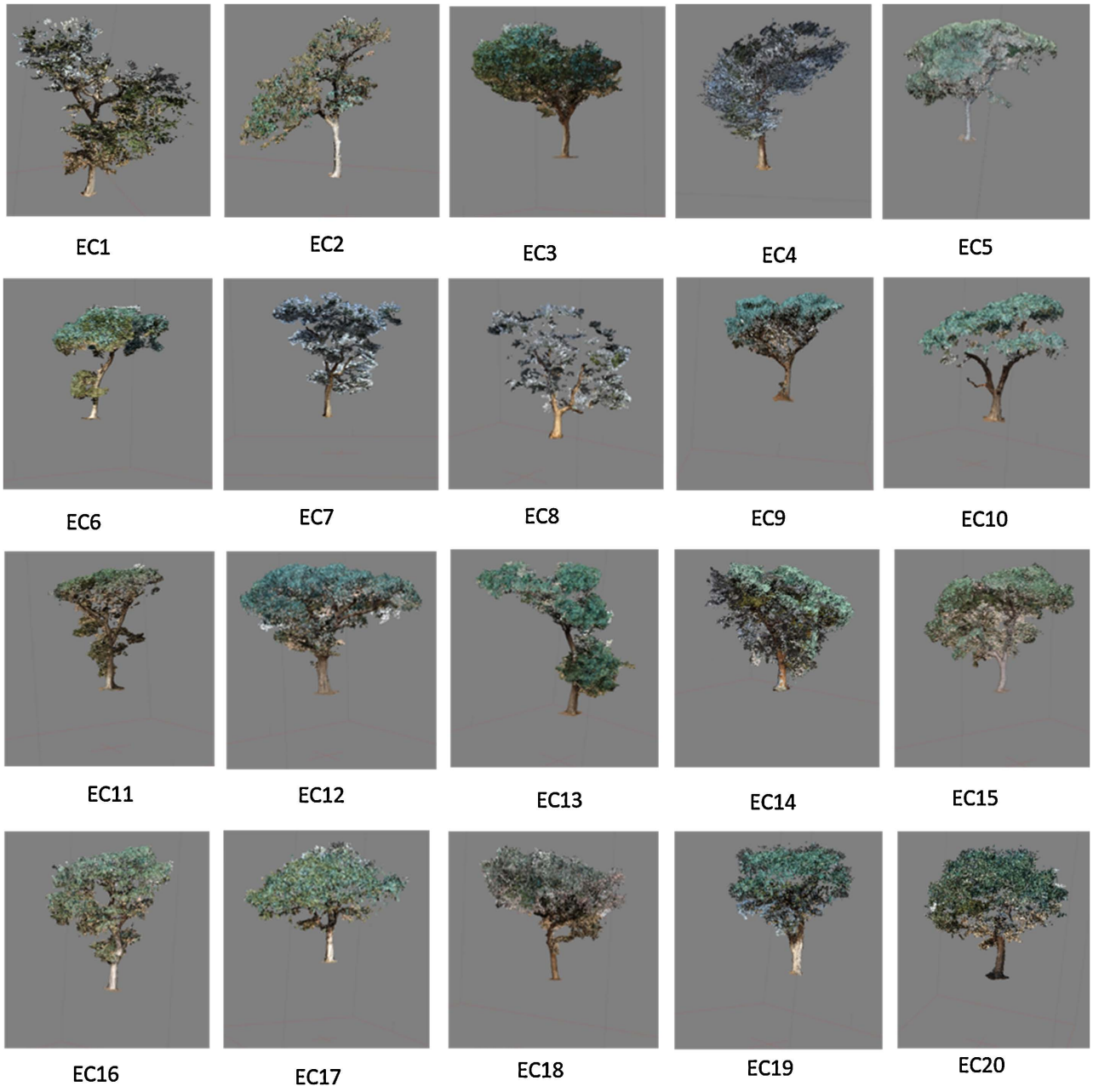


**Figure A1.** 3D Models of the 20 Sampled Individuals of *Faidherbia albida.*

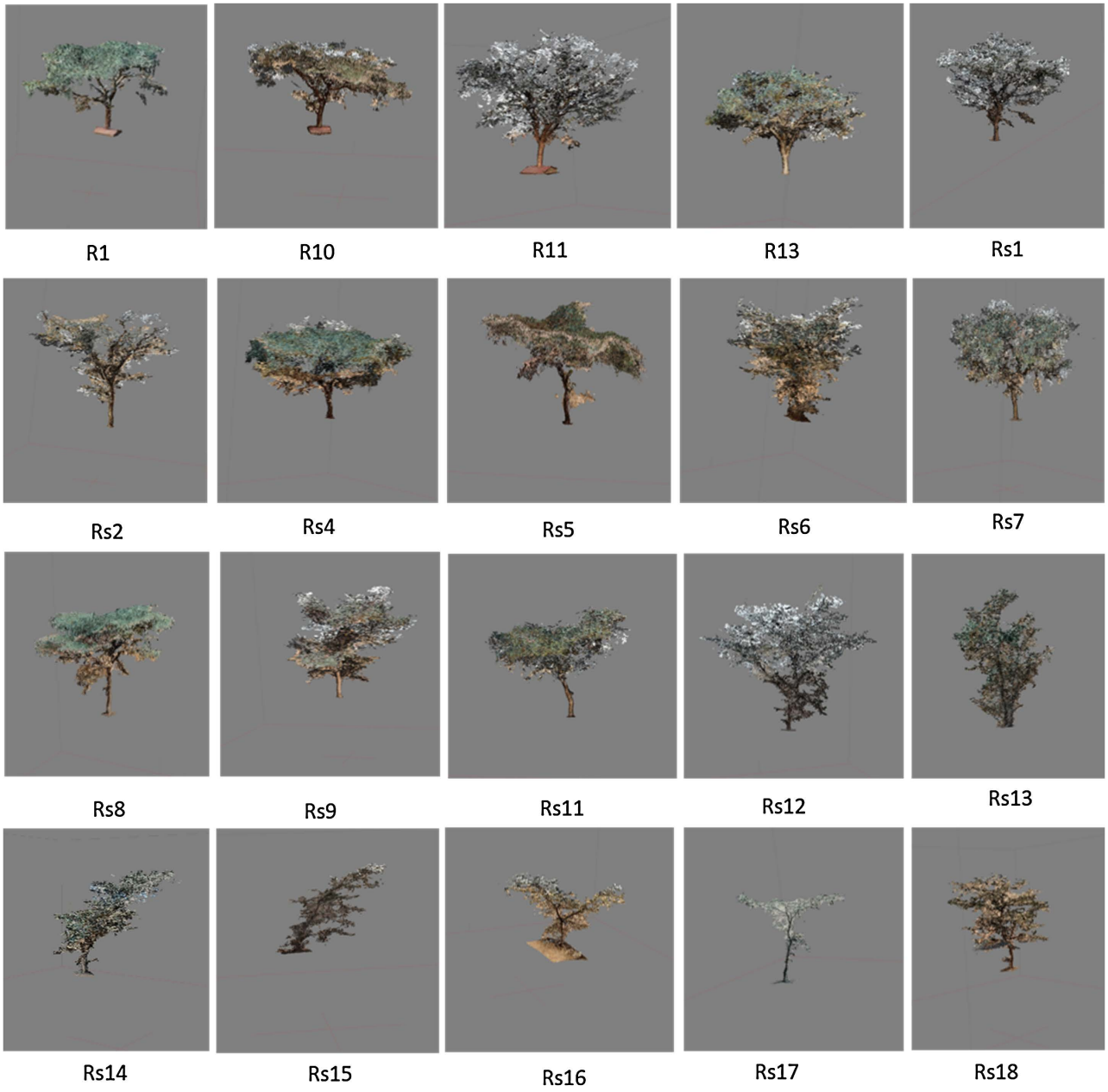


**Figure A2.** 3D Models of the 20 Sampled Individuals of *Acacia tortilis.*

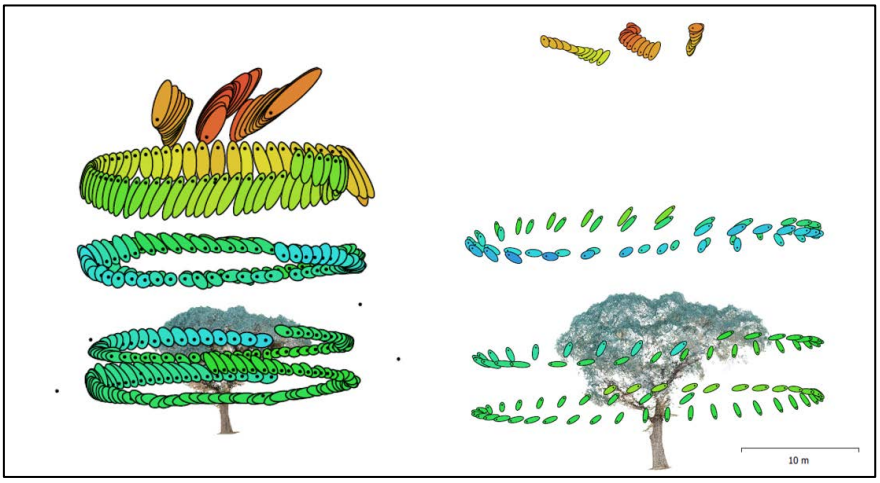


**Figure A3.** Example of camera positions and error estimates for tree EC12. Z-error is represented by the color of the ellipse, while X and Y errors are represented by the shape of the ellipse. Estimated camera positions are indicated by black dots.

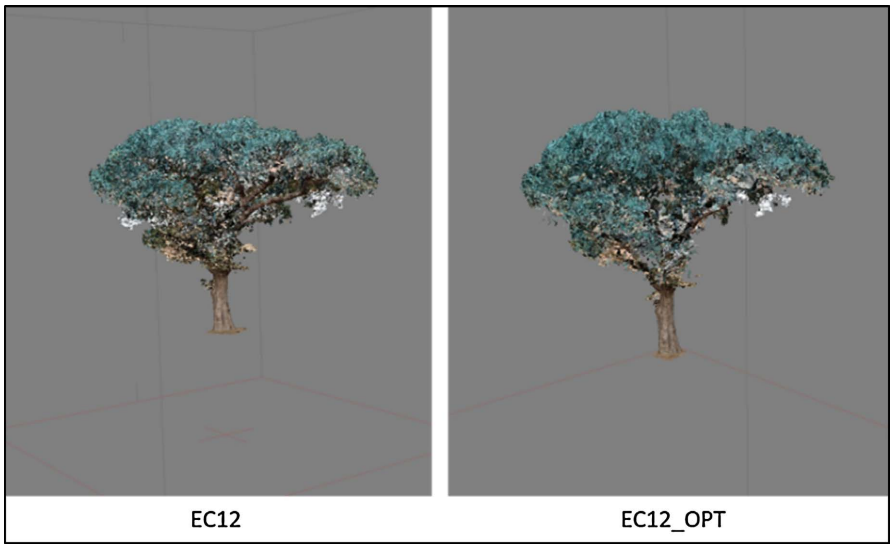


**Figure A4.** 3D model example from the non-optimized protocol (EC12) and model from the optimized protocol (EC12_OPT).

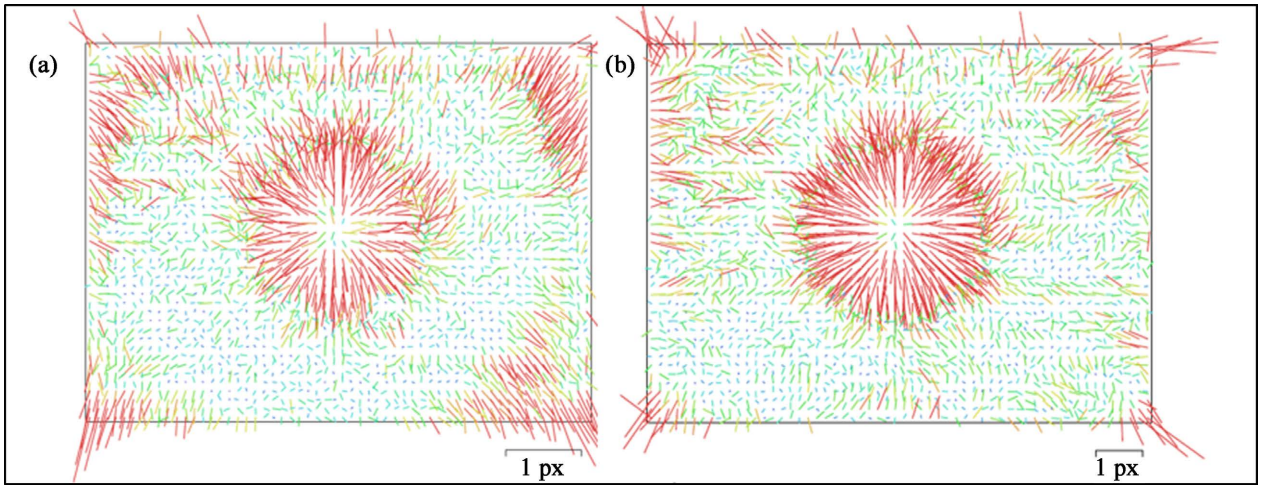


**Figure A5.** Residuals of tie points for the original (a) and the EC12 optimized model (b)

**Table A1.** Distribution of images per individual. EC refers to *Faidherbia albida*; R and Rs refers to *Acacia raddiana.*

| Drone | Ground images | Drone and ground images |
|---|---|---|
| EC1, EC2, EC5, EC6, EC10, EC3, EC9, EC12, EC13, EC15, EC16, EC17, EC18, EC20, R1, R10, R13, Rs2, Rs4, Rs5, Rs6, Rs7, Rs8, Rs9, Rs10, Rs11, Rs12, Rs13, Rs17, Rs18 | EC4, EC7, EC8, R11, Rs15, Rs16 | EC11, EC14, EC19, Rs14 |